

Histopathological changes of Quercetin on internal organs against *Klebsiella pneumoniae* in Mice

Ikram A. Al Sammaraa*, Roua J. Mohammed*, Haider Mohammed Ali Al-Rubaie**, Layth Abdulmajeed Abdulkahle***

*Department of Microbiology, College of Veterinary Medicine, University of Baghdad, Iraq
, *Department of Pathology, College of Veterinary Medicine, University of Baghdad, Iraq

Corresponding author: ikram@covm.uobaghdad.edu.iq

ORCID: https://orcid.org/0000_0003_4895_9926

https://orcid.org/0000_0001_5931_8855

Important dates: Received: 01-November-2025; Accepted: 10- March-2026; Published: March-2026

Abstract

Background: Quercetin is a natural flavonoid present in fruits and medicinal herbs with antioxidant, anti-inflammatory, and antimicrobial properties. It modulates immune responses and protects tissues from oxidative and infectious insults. *Klebsiella pneumoniae* is a Gram-negative bacterium and a significant cause of pneumonia and septicemia, and its increasing resistance requires effective natural adjunctive treatments. **Aims:** The current study evaluated the histopathological impact of quercetin on internal organs in mice experimentally infected with *K. pneumoniae*. Forty Swiss mice were divided into groups treated with quercetin at 150, 100, and 50 mg/ml once weekly for six weeks, and a control group received PBS. All animals were challenged intraperitoneally with *K. pneumoniae* (1.5×10^8 CFU/ml). Seven days later, spleen, liver, lung, and intestine were collected, fixed in 10% formalin, and histologically examined. **Results:** Pre-challenge quercetin-treated groups showed lymphoid hyperplasia and megakaryocytic activation in the spleen, indicating immune stimulation. Treated mice after infection had reduced splenic hypoplasia, hepatic mild degeneration instead of diffuse necrosis, and preserved alveolar and intestinal architecture. Intestinal villi were truncated but with preserved mucosal integrity and reduced lymphocytic infiltration compared to infected controls. **Conclusion:** Quercetin exhibited a biphasic immunomodulatory and tissue-protective effect—pre-infection stimulation of immune readiness and post-infection attenuation of inflammation and necrosis. These findings sanction its antioxidant and anti-inflammatory roles and suggest

Keyword: Quercetin; *Klebsiella pneumoniae*; Histopathology; Immunomodulation; Iraq



This is an open access article licensed under a [Creative Commons Attribution-Noncommercial 4.0 International License](https://creativecommons.org/licenses/by-nc/4.0/).

Introduction

Quercetin, a flavonoid from fruits, vegetables, and medicinal plants, has received considerable attention due to its diverse pharmacological properties like antioxidant, anti-inflammatory, and antimicrobial activities (Li *et al.*,2016; Wang *et al.*,20220). It has been reported to modulate inflammatory pathways, inhibit cytokine overproduction, and protect tissues from structural damage (Cushnie & Lamb,2011; Zhang *et al.*,2016)

Its histoprotective effects have been documented in different experimental models. It has the capacity to reduce hepatic fibrosis, protect lung tissue from inflammatory injury, and maintain intestinal mucosal integrity against infective and chemical insults (Han *et al.*,2021; Vithalkar *et al.*,2025). In Iraq, several studies have highlighted its tissue protection effect in different injurious conditions. For example, a study at the University of Baghdad determined that quercetin improved liver, heart, and duodenal inflammation and degeneration in iron-overloaded rabbits compared to untreated controls (Awad & Al-Okaily,2023). Quercetin also protected the liver against acute Cyclophosphamide-induced toxicity, improving both biochemical enzyme markers and histological integrity (Ismail *et al.*,2023). Additionally, co-administration of quercetin along with hepatotoxic agents, Isoniazid and Rifampicin, counteracted the elevation of liver enzymes and tissue injury (Qader *et al.*,2014). Collectively, all these findings serve to bear witness to the uniform nature of the protective action of quercetin on different organs against inflammation and tissue injury under diverse noxious conditions.

A Gram-negative opportunistic bacterium called *Klebsiella pneumoniae* causes liver abscesses, septicaemia, pneumonia, and UTIs, especially in those with weakened immune systems (Navon-Venezia *et al.*, 2017) Infection is usually accompanied by necrosis, blood vessel congestion, and immune cell infiltration in vital organs (Arrazuria *et al.*,2022). With the rise of multidrug-resistant strains, natural compounds such as quercetin have gained prominence as adjuvant therapeutic molecules. The present research is planned to evaluate the histopathological changes in the major organs of experimentally infected mice with *K. pneumoniae* and to investigate quercetin's protective role according to its documented anti-inflammatory and tissue-protective properties. This study is complementary to that of (Al-Sammaraae ,2025) where it was demonstrated that quercetin significantly affects the levels of proinflammatory cytokines in *K. pneumoniae* infected mice, thereby establishing its therapeutic potential as an additive agent. The current study aims to further elaborate on these findings by connecting cytokine modulation with histopathological alterations of vital organs for a clearer understanding of the defense mechanisms of quercetin against *K. pneumoniae* caused damage.

Material and methods

Ethical approval

On March 24, 2024, ethical approval was given by the local committee of animal care and use at the University of Baghdad's College of Veterinary Medicine, number P-G/649.

Bacterial strain:

K. pneumoniae strain was sourced from the Microbiology Department at the College of Veterinary Medicine. The strain was initially transferred from brain heart infusion broth containing 15% glycerol, followed by subculturing on MacConkey agar and incubating for 24 hours at 37°C. Subsequently, the strain was inoculated into mice to obtain a fully encapsulated virulent form. The virulent organisms were then isolated from the organs of the mice and streaked onto MacConkey agar, which was incubated for an additional 24 hours at 37°C. Growth was monitored, and purity was verified through Gram staining (Hadi & Aldujaili, 2022).

Preparation for Quercetin:

Quercetin was made in three distinct concentrations: 150 mg/ml, 100 mg/ml, and 50 mg/ml. It was obtained as a dietary supplement (AMAZING AN NUTRITION, 500 mg).

Infectious dosage:

Using three bacterial concentrations (1.5×10^8 , 3.0×10^8 , and 6.0×10^8 cfu/ml), the infectious dosage (pilot study) was made using the McFarland tube method on a total of 24 mice split into three groups of eight mice each. 1.5×10^8 cfu (0.1 ml orally) was given to Group 1, 3.0×10^8 cfu (0.1 ml orally) was given to Group 2, and 3.0×10^8 cfu (0.1 ml orally) was given to Group 3. The infectious dose was 1.5×10^8 cfu/mL, and fatality rates and clinical signs were tracked for three days after infection.

Experimental Animals:

Forty Swiss mice, ten in each of the four groups, were used in the study. The animals included both male and female mice. For six weeks, the first, second, and third groups received oral quercetin at doses of 150, 100, and 50 mg/ml, respectively, once a week. As a negative control, the fourth group received 1 ml of PBS. After six weeks, all animals received an infectious dose of *K. pneumoniae* (1.5×10^8 cfu/ml, I.P.).

Histopathological Analysis

Mice were put to sleep for histopathological analysis after a week of the challenge, and their internal organs—liver, spleen, gut, and lung—were removed, promptly preserved in a 10% formalin solution, and sectioned in accordance with (Luna, 1968).

Results

Histopathological changes:

After a week of exposure to an infectious dose of *K. pneumonia* (1.5×10^8 cfu), histological assessments indicated distinct histopathological alterations across the studied groups.

Group 1 (after 60 days with quercetin 150 mg/ml): The spleen exhibited significant hyperplasia of lymphoid follicles within the white pulp, alongside pronounced sinusoidal dilation and congestion in the red pulp. There was also notable proliferation of megakaryocytes (Figure 1). In the small intestine, histopathological examination revealed normal mucosal villi, enterocytes, and intestinal glands (Figure 2). The lung histopathology (G1-before) showed mild interstitial pneumonia characterized by considerable proliferation of bronchial-associated lymphoid tissue, alveolar emphysema, and thickened interstitial tissue associated with infiltration of mononuclear leukocytes (MNLs), and vascular congestion (Figure 3). The liver showed portal vein dilation and congestion with marked perivascular cuffing of lymphocytes (Figure 4)

Group 1 (after 7 days post-infection): The spleen displayed marked hypoplasia of lymphoid follicles in the white pulp, while the red pulp showed significant sinusoidal dilation, congestion, and proliferation of megakaryocytes, along with hyperplasia of lymphoid cells within the splenic cords (Figure 5). The small intestine showed normal villus lining cells and normal intestinal glands (Figure 6). The lung presented a normal structure of the pulmonary interstitium, blood vessels, bronchial segments, and alveoli (Figure 7). In the liver, there was notable dilation of both the central and portal veins, with minimal perivascular lymphocytic aggregation. The hepatic cords exhibited mild generalized cellular swelling (Figure 8).

Group 2 Observations After 60 Days Post Quercetin Administration (100 mg/ml): The spleen exhibited normal lymphoid follicles within the white pulp, alongside mild sinusoidal dilation and congestion in the red pulp (Figure 9). The lungs displayed signs of mild interstitial pneumonia, characterized by thickening of the interstitial tissue due to infiltration of mononuclear leukocytes (MNLs), vascular congestion, intra-alveolar transudation, and mild emphysema (Figure 10). In the small intestine, significant enteritis was observed, marked by thickening of the mucosal villi linked to leukocyte infiltration, as well as necrosis of enterocytes and atrophy of intestinal glands (Figure 11). The liver showed notable perivascular lymphocytic aggregation accompanied by zonal degeneration of the hepatic cords, which presented mild cellular swelling (Figure 12). **Group 2 Observations After 7 Days Post Infection:** The spleen exhibited significant atrophy and hypoplasia of the lymphoid follicles, along with hypoplasia of the splenic cords within the red pulp (Figure 13). The lungs appeared normal, with intact pulmonary interstitium, blood vessels, bronchial

segments, and alveoli (Figure 14). The small intestine demonstrated mild hyperplasia of the villous enterocytes, with normal villi and intestinal glands (see Figure. 15). The liver showed considerable dilation of both the central and portal veins, accompanied by perivascular lymphocytic cuffing. The hepatic cords indicated generalized mild degeneration along with hepatocyte necrosis (Figure 16).

Group 3 Observations after 60 Days Post-Administration (Quercetin 50 mg/ml): The spleen exhibited normal lymphoid follicles within the white pulp, alongside mild sinusoidal dilation coupled with congestion in the red pulp (Figure 17). The lungs displayed mild interstitial pneumonia, characterized by thickening of the interstitial tissue due to infiltration by mononuclear leukocytes (MNLs), along with vascular congestion and slight emphysema (Figure 18). The small intestine showed normal mucosal villi and intestinal glands (Figure 19). In the liver, there was significant perivascular lymphocytic aggregation and zonal degeneration of the hepatic cords, which indicated mild cellular swelling (Figure 20).

Group 3 Observations after 7 Days Post-Infection: The spleen revealed significant atrophy, with hypoplasia of the lymphoid follicles and pronounced hypoplasia of the splenic cords within the red pulp (Figure 21). The small intestine showed normal appearance of mucosal villi with normal enterocytes (Figure.22). The lungs presented with normal pulmonary interstitium, blood vessels, and bronchial segments, along with associated diffuse lymphoid tissue and alveoli (Figure 23). The liver showed an irregularly dilated central vein with marked perivascular lymphocytic cuffing, alongside zonal degeneration and necrosis of the hepatic cords, featuring infiltrated mononuclear leukocytes (Figure 24).

Group 4 Positive Control Observations after 7 Days Post-Infection: The spleen exhibited a severe sago spleen appearance, with amyloid deposition around the lymphoid follicles, hypoplasia of the lymphoid follicles in the white pulp, and reduced splenic cord lymphoid tissue (Figure 25). The lungs maintained normal interstitial tissue, alveoli, and bronchial segments (Figure 26). The small intestine displayed normal mucosal villi with evidence of enterocyte hyperplasia and intact intestinal glands (Figure 27). The liver demonstrated minimal perivascular lymphocytic aggregation, irregularly dilated portal vein, and severe zonal degeneration with necrosis of the hepatocytes (Figure 28).

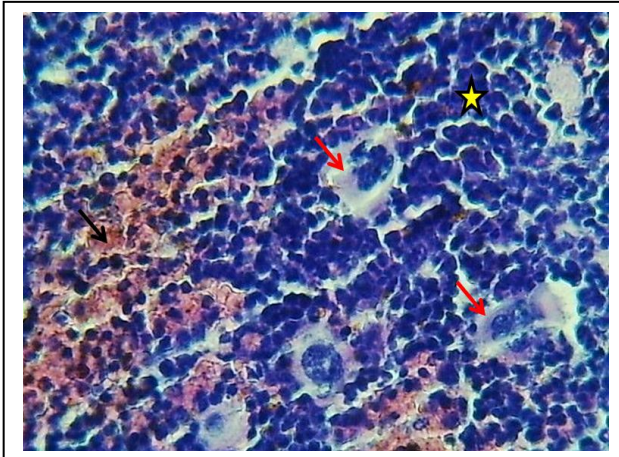


Figure 1: section of spleen (G1-before) shows marked hyperplasia of lymphoid tissue within white pulp (Asterisks) & marked sinusoidal dilation with congestion of red pulp (Arrows) and proliferation of megakaryocytes. H&E. 400x

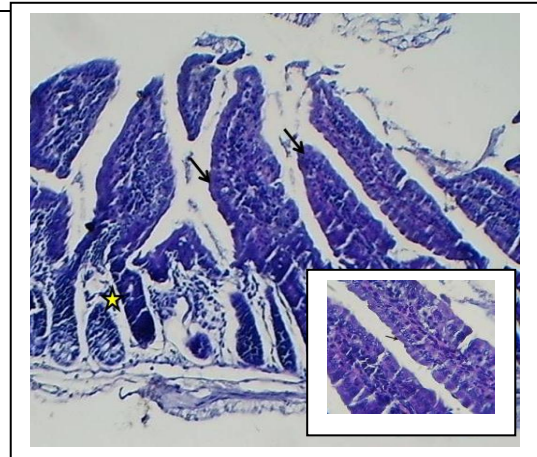


Figure 2: section of small intestine (G1-before) shows normal appearance of mucosal villi with normal enterocytes (arrows) & intestinal glands (Asterisk). H&E stain. 100x & 400x

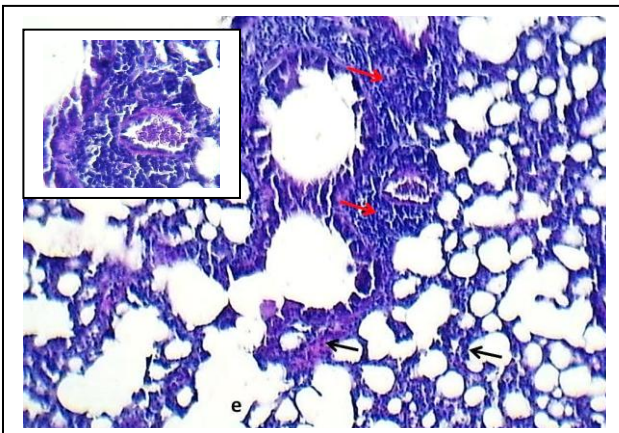


Figure 3: section of lung (G1-before) mild interstitial pneumonia revealed marked proliferation of bronchial associated lymphoid tissue (Red arrows), alveolar emphysema (e) and thickening of interstitial tissue related with infiltration of MNLs and congestion (Black arrows). H&E stain. 100x & 400x

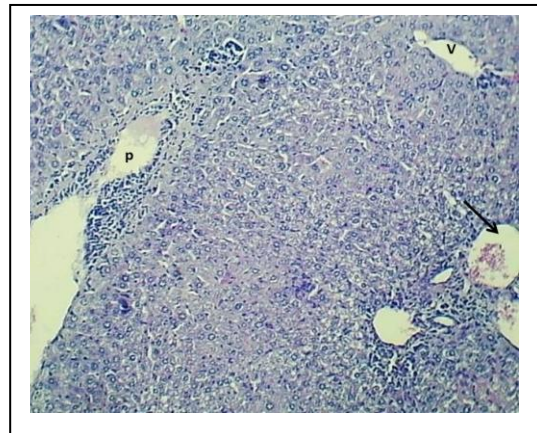


Figure 4: section of liver (G1 before) shows: marked dilation of portal vein (P) and congestion (Arrow) with marked peri vascular cuffing of lymphocytes. H&E stain. 100x & 400x

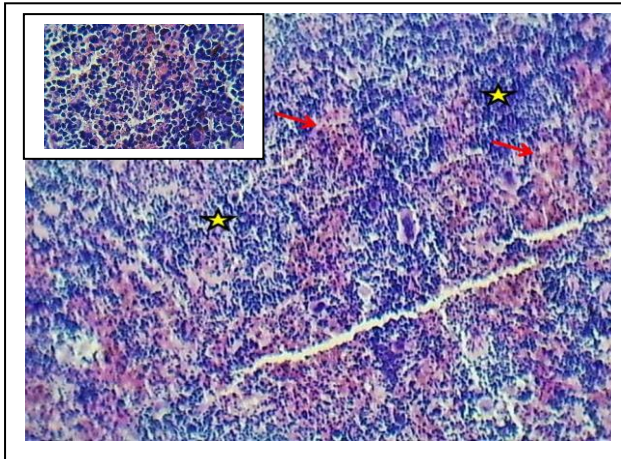


Figure 5: section of spleen (G1-after) shows marked hypoplasia of lymphoid tissue (Asterisks) with marked sinusoidal dilation with congestion (Arrows) and proliferation of megakaryocytes.H&E.100x&400x

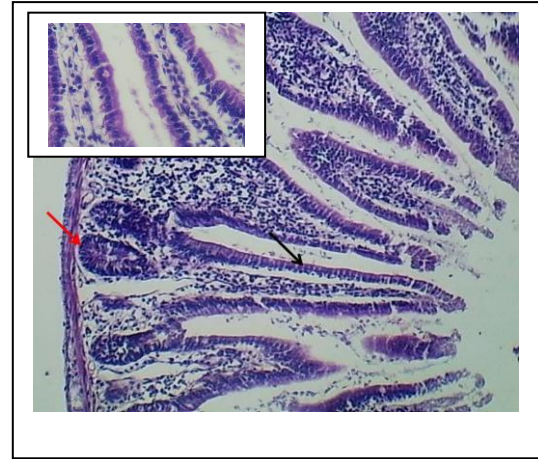


Figure 6: Section of intestine (G1 after) shows: normal villus lining cells (black arrow) & normal intestinal gland (red arrow). H&E stain. 100x&400x

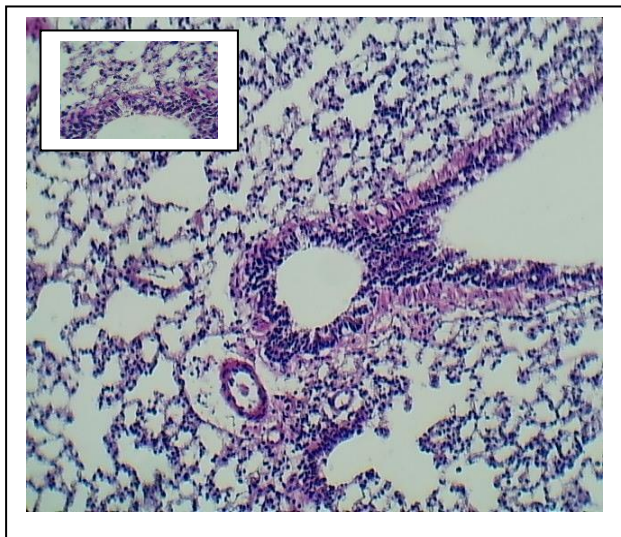


Figure 7: section of lung (G1-after) normal interstitial tissue, normal bronchial segment, blood vessels and alveoli. H&E stain.100x&400x

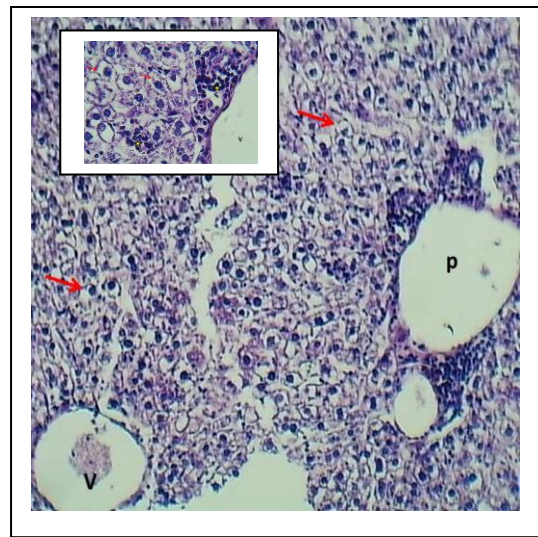


Figure 8: Section of liver (G1-after) shows: marked dilation of central vein (V) and portal vein (P), with little perivascular lymphocytic aggregation, the hepatic cords revealed mild cellular swelling (Arrow). H&E stain. 100x&400x

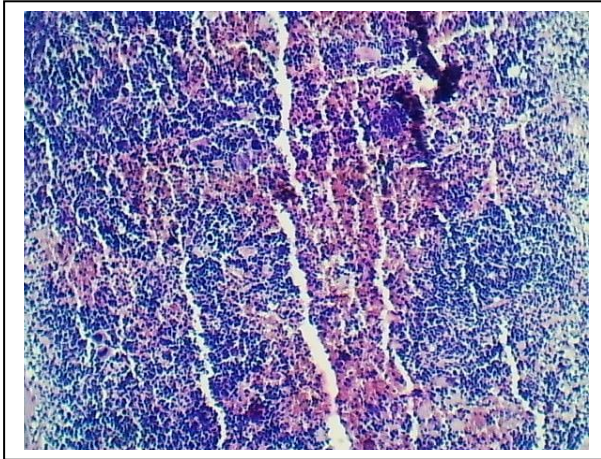


Figure 9: section of spleen (G2-before) shows normal appearance of lymphoid follicles with mild sinusoidal dilation with congestion (Arrows).H&E.100x&400x

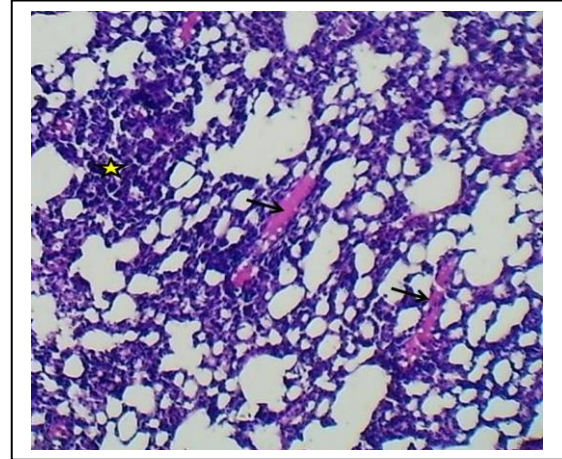


Figure 10: section of lung (G2-before) mild interstitial pneumonia (asterisk), and alveolar transudate (arrows). H&E stain.100x&400x



Figure 11: section of intestine (G2-before) marked enteritis revealed thickening of mucosal villi associated with infiltration of leukocytes (Arrows) with necrosis of enterocytes and necrosis with atrophy of intestinal glands (Asterisks). H&E stain.100x.

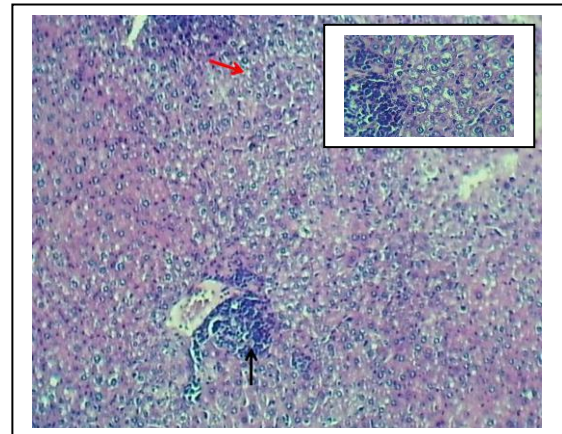


Figure 12: Section of liver (G2-before) shows: perivascular lymphocytic aggregation (black arrow) and zonal degeneration of the hepatic cords that revealed mild cellular swelling (Red arrow). H&E stain. 100x&400x

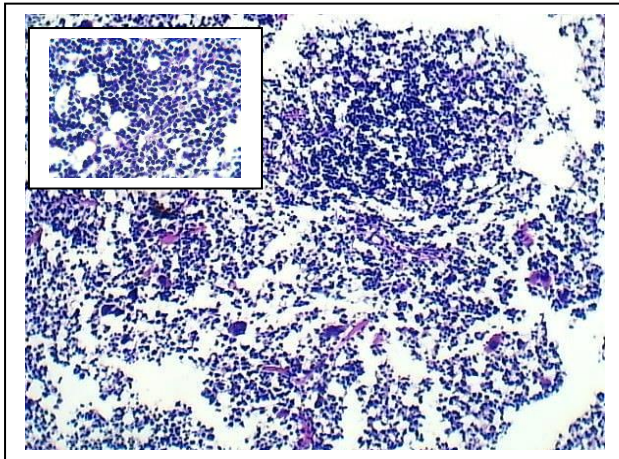


Figure 13: section of spleen (G2-after) shows marked atrophy with hypoplasia of lymphoid follicles hypoplasia of splenic cords within red pulp.H&E.100x&400x

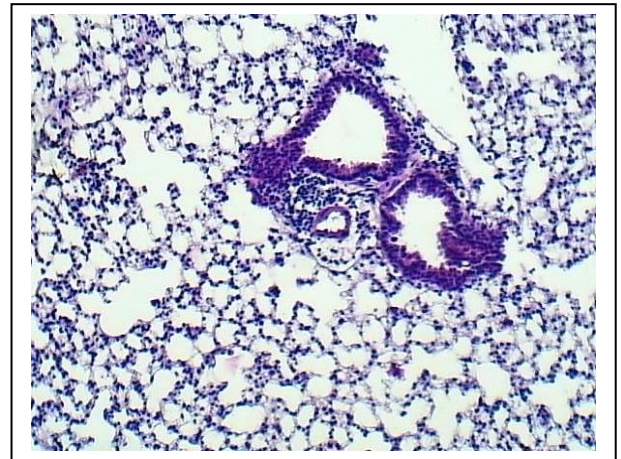


Figure 14: section of lung (G2-after) showed bronchial segments, blood vessels and alveoli. H&E stain.100x.

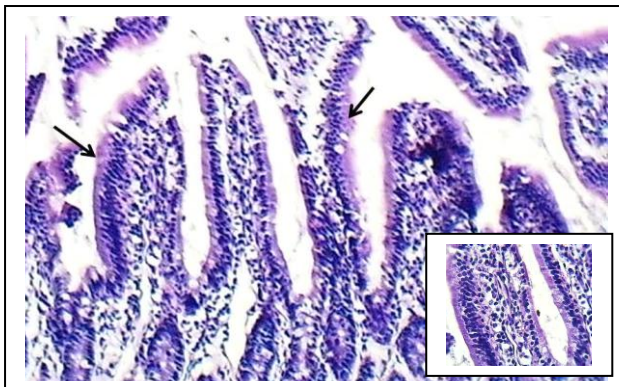


Figure 15: section of small intestine (G2-after) mild hyperplasia of villous enterocytes (arrows) with normal villi and intestinal glands. H&E stain.100x&400x

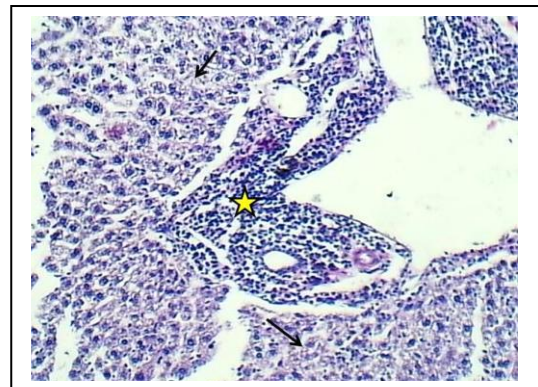


Figure 16: Section of liver (G2-after) shows: perivascular lymphocytic cuffing (asterisk) and zonal degeneration of the hepatic cords revealed (arrow). H&E stain. 100x&400x

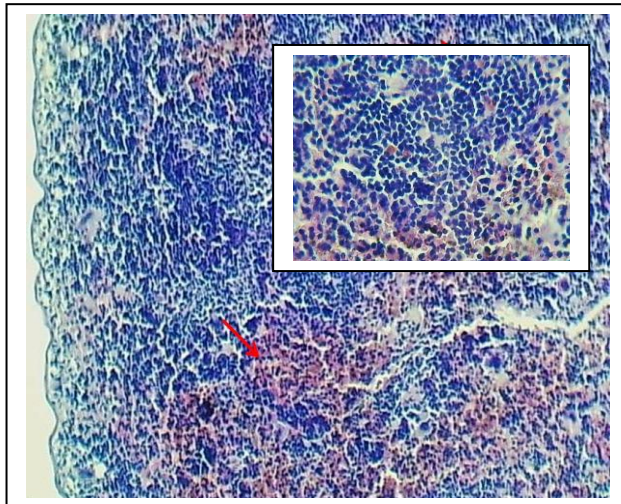


Figure 17: section of spleen (G3-before) shows normal appearance of lymphoid follicles with mild sinusoidal dilation with congestion (Arrows).H&E.100x&400x

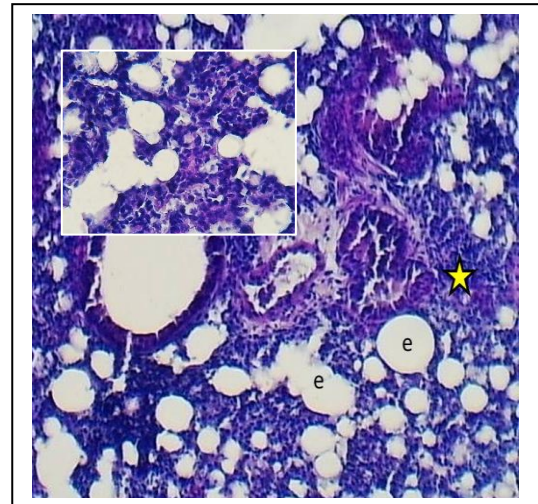


Figure 18: section of lung (G3-before) severe interstitial pneumonia (asterisk) with alveolar emphysema (e) and alveolar congestion (arrow). H&E stain.100x &400x

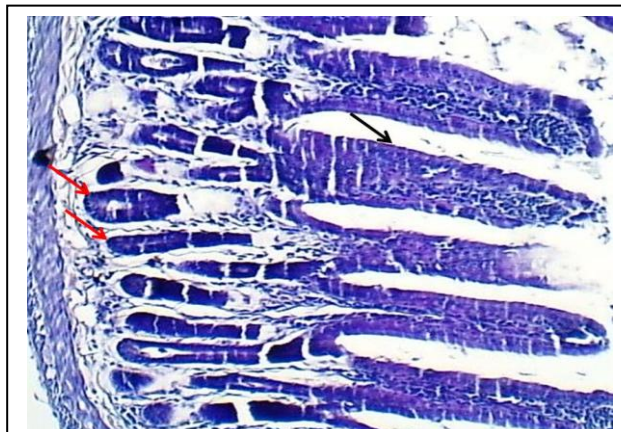


Figure 19: section of intestine (G3-before) normal of mucosal villi (black arrows) and normal intestinal glands (Asterisks). H&E stain.100x.

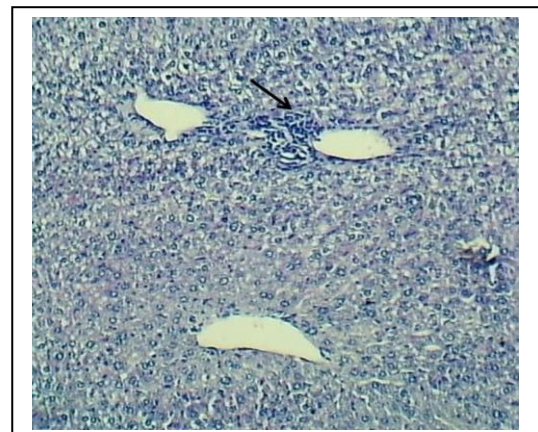


Figure 20: Section of liver (G3-before) shows: little perivascular lymphocytic aggregation (arrow) and little zonal degeneration of the hepatic cords that revealed mild cellular swelling. H&E stain. 100x and 400 x.

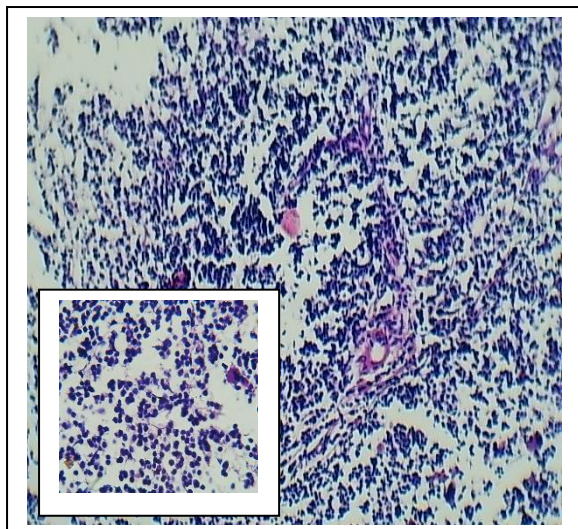


Figure 21: section of spleen (G3-after) shows marked atrophy with hypoplasia of lymphoid follicles hypoplasia of splenic cords within red pulp. H&E. 100x&400x



Figure 22: section of small intestine (G3-after) shows normal appearance of mucosal villi with normal enterocytes (arrows) & intestinal glands (Asterisk). H&E stain. 100x

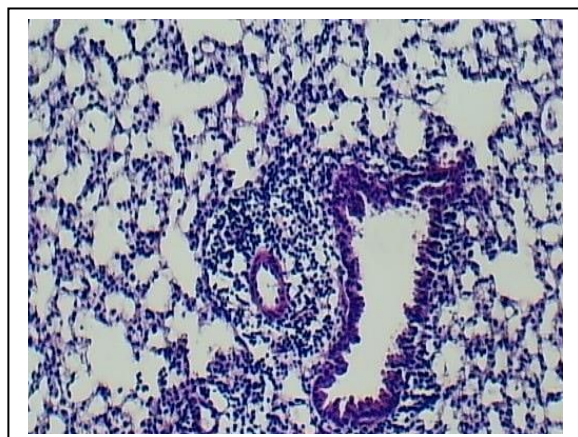


Figure 23: section of lung (G3-after) showed normal bronchial segments, with normal related lymphoid tissue, normal blood vessels and alveoli. H&E stain. 100x&400x

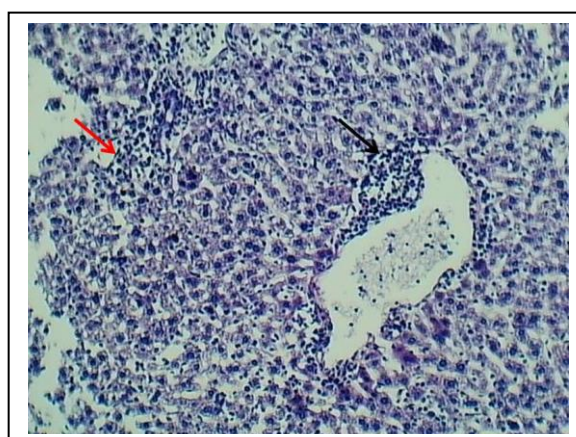


Figure 24: Section of liver (G3-after) shows: irregularly dilated central vein with marked perivascular lymphocytic cuffing (black arrow) and zonal degeneration with necrosis of the hepatic cords (red arrow). H&E stain. 100x&400x

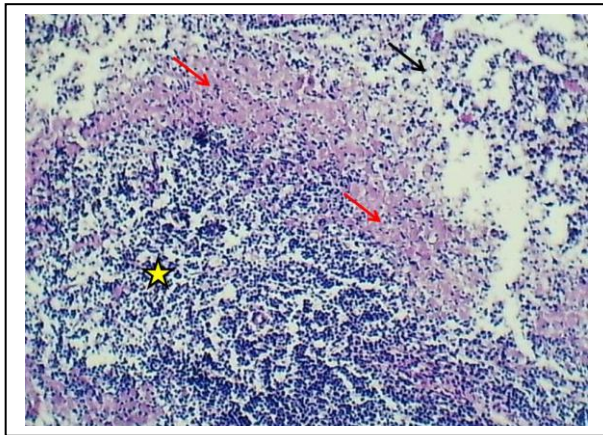


Figure 25: section of spleen (G4) shows severe appearance sago spleen that revealed peri lymphoid follicle deposition of amyloid (Red arrow), hypoplasia of lymphoid follicles with white pulp (Asterisk) & hypoplasia of lymphoid tissue of splenic cords (black arrows).H&E.100x&400x

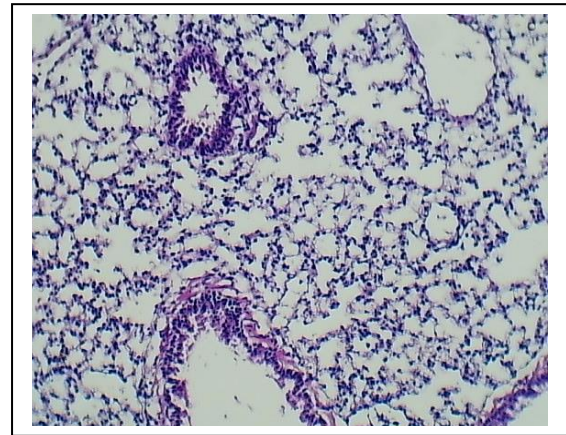


Figure 26: section of lung (G4) normal interstitial tissue (asterisk), normal alveoli (e) and bronchial segments. H&E stain.100x.

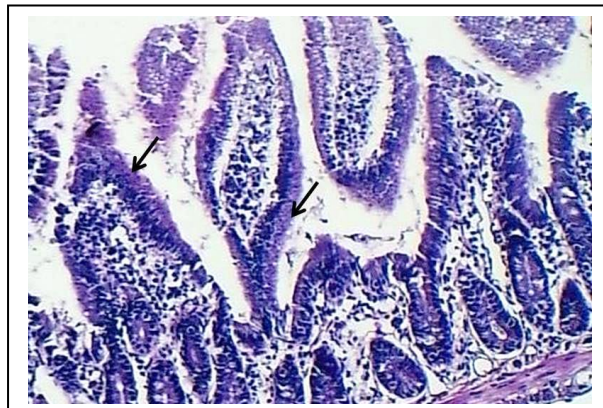


Figure 27: section of intestine (G4) normal of mucosal villi with marked hyperplasia of enterocytes (black arrows) and normal intestinal glands. H&E stain.100x.

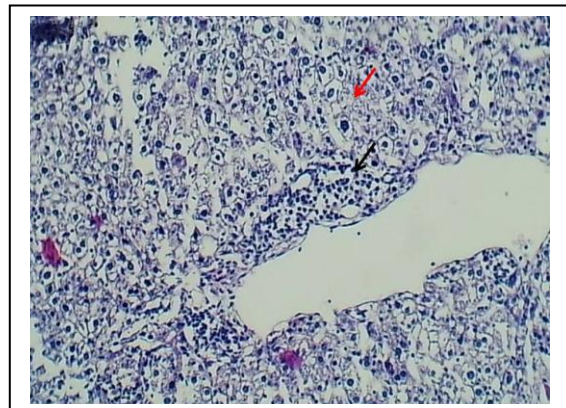


Figure 28: Section of liver (G4) shows: perivascular lymphocytic aggregation with irregularly dilated portal vein (black arrow) and severe zonal degeneration with necrosis of the hepatocytes. H&E stain. 100x.

Discussion:

The present study investigated the histopathological effect of quercetin on spleen, liver, and lung tissues of mice infected with *Klebsiella pneumoniae*. The findings indicate that quercetin exerted a two-way modulatory effect, enhancing preparedness of the immune system prior to infection as well as lowering tissue damage subsequent to bacterial challenge.

Spleen:

Severe lymphoid hyperplasia and megakaryocytic proliferation in the high-dose group prior to challenge suggest that quercetin may be an immunostimulant. This corroborates the previously reported activity of stimulating lymphocyte proliferation as well as immune response modulation (Li *et al.*, 2016). Splenic hypoplasia, on the other hand, has been observed after bacterial infection, where it may result from migration of lymphocytes into peripheral tissues or apoptosis resulting from activation. The same biphasic immune stimulation succeeded by depletion in tissues has also been documented in immunomodulatory agent experiment (Boots *et al.*, 2008). The same outcomes have been reported in Iraqi studies, where quercetin controlled immune and inflammatory activities in animal models, confirming its immunomodulatory function (Mohammed, 2025)

Liver:

The liver of quercetin-treated mice showed mild periportal inflammation and hepatocellular degeneration, whereas infected untreated controls showed increased necrosis. Systemic bacterial infection-induced liver injury is mainly mediated through lipopolysaccharide (LPS)-induced inflammation and oxidative stress (Riwu *et al.*, 2022). The reduced necrosis in quercetin groups reflects its hepatoprotective action, which agrees with its antioxidant and anti-inflammatory activity (Chen *et al.*, 2016). These protective hepatic effects of quercetin have also been demonstrated in Iraqi studies on drug-induced hepatotoxicity, where structural damage was decreased and biochemical markers were increased by quercetin in rat models (Obead *et al.*, 2025; Awad & Al-Okaily, 2023). These local findings contribute to the evidence that quercetin preserves hepatocyte architecture from different insults, e.g., infections and xenobiotics.

Lungs:

Quercetin-treated mice exhibited comparatively intact alveolar structures with minimal congestion prior to bacterial challenge. Following infection, pulmonary damage was observed but less severe than in untreated controls. This observation is supported by global evidence showing that quercetin reduces neutrophil infiltration, NF- κ B activation, and pro-inflammatory cytokine production in models of pneumonia and endotoxin-induced lung injury (Huang *et al.*, 2024). (Ismail *et al.*, 2023) in Iraq established that quercetin enhanced the histopathological changes in benzene inhalation-exposed lungs, confirming its protective role against pulmonary tissue from inflammatory or toxic damage.

Intestine:

Histopathological alterations in the quercetin-treated groups' intestine were shortening of villi, vascular congestion, and lymphocytic infiltration of the lamina propria with variable severity depending on dose and infection. In the positive control group, there were more severe lesions such as villous atrophy and desquamation of epithelium. The findings suggest that systemic *Klebsiella pneumoniae* infection compromises the intestinal architecture through endotoxin-mediated inflammation, increased permeability, and recruitment of immune cells into the mucosa. The milder changes observed in quercetin-treated animals indicate that quercetin has a protective effect on the intestinal mucosa. This can be attributed to its antioxidant activity, inhibition of NF- κ B-mediated inflammation, and integrity of tight junction proteins, which all contribute to villous integrity and diminish epithelial damage (Li *et al.*,2016; Riwu *et al.*,2022). The dose-related protection in the current study also contributes to evidence that quercetin at higher concentrations more potently reduces mucosal injury.

These results are consistent with international data that quercetin supplementation suppresses intestinal inflammation and maintains villous height in either infection or chemically induced models (Luna,1968; Mohammed,2025). Iraqi research also supports this result: (Awad & Al-Okaily,2023) demonstrated the potential of quercetin in enhancing duodenal histopathological damage in iron overload models, and (Chen *et al.*,2016) demonstrated its potential in preserving intestinal structure and reducing apoptosis in drug-induced damage. Both Iraqi and international research combined highlight the potential of quercetin in protecting the gastrointestinal tract from diverse insults, such as bacterial infection.

Conclusion:

Quercetin also exhibited excellent histopathological protection against *Klebsiella pneumoniae* infection in mice, particularly in the spleen, liver, lungs, and intestine. Its mechanism appears to be two-pronged: stimulating lymphoid tissue at basal levels but inhibiting overshooting inflammation and tissue damage upon infection. Quercetin inhibited necrosis of the liver, reduced pulmonary consolidation, preserved villous integrity in the intestine, and diminished splenic exhaustion. These actions are consistent with findings from international as well as Iraqi research studies, which report antioxidant, anti-inflammatory, and immunomodulatory actions of quercetin. Therefore, quercetin may serve as a valuable therapeutic adjuvant to conventional antimicrobial treatment, although extensive clinical and experimental research are required to define its effectiveness and ideal dosage in infectious diseases.

Recommendations

It is recommended that further studies be conducted to elucidate the molecular mechanisms involved in the protective effects of quercetin in a *Klebsiella pneumoniae* infection

model. Additionally, the potential for combined use of quercetin with conventional antimicrobial therapy and the determination of the optimal therapeutic dose could further define its clinical utility.

Acknowledgment

The authors would like to thank the College of Veterinary Medicine, University of Baghdad, for providing the facilities and support necessary for conducting this study. The authors would also like to thank the Department of Microbiology for providing the bacterial strain and the Department of Pathology for their assistance in the histopathological examinations. The authors would also like to thank the technical staff of the Department of Microbiology for their assistance in conducting this study.

Author Contributions:

Ikram A. Al Sammaraa was responsible for the conceptualization, supervision, and overall project design. Roua J. Mohammed contributed to the methodology, data collection, and initial draft preparation. Haider Mohammed Ali Al-Rubaie performed the histopathological examination and data analysis. Layth Abdulmajeed Abdulkahle contributed to data interpretation, manuscript revision, and final approval of the submitted version. All authors have read and approved the final manuscript.

Conflict of Interest:

The authors declare no conflict of interest.

Reference:

- Al-Sammaraa, I. A. A. (2025). Evaluation of quercetin on proinflammatory cytokines against *Klebsiella pneumoniae** in mice. *Biomedical and Pharmacology Journal, 18*(3).
- Arrazuria, R., Kerscher, B., Huber, K. E., Hoover, J. L., Lundberg, C. V., Hansen, J. U., et al. (2022). Variability of murine bacterial pneumonia models used to evaluate antimicrobial agents. *Frontiers in Microbiology*, 13*, 988728. <https://doi.org/10.3389/fmicb.2022.988728>
- Awad, M. A., & Al-Okaily, B. (2023). Histopathological changes of heart, liver, and duodenum in iron overload: Comparing the role of quercetin with deferoxamine. *Iraqi Journal of Veterinary Medicine, 47*(2), 117–124. <https://doi.org/10.30539/5kcacw03>
- Boots, A. W., Haenen, G. R., & Bast, A. (2008). Health effects of quercetin: From antioxidant to nutraceutical. *European Journal of Pharmacology, 585*(2–3), 325–337. <https://doi.org/10.1016/j.ejphar.2008.03.008>

- Chen, S., Jiang, H., Wu, X., & Fang, J. (2016). Therapeutic effects of quercetin on inflammation, obesity, and type 2 diabetes. **Mediators of Inflammation*, 2016*, 9340637.
<https://doi.org/10.1155/2016/9340637>
- Cushnie, T. P. T., & Lamb, A. J. (2011). Recent advances in understanding the antibacterial properties of flavonoids. **International Journal of Antimicrobial Agents*, 38*(2), 99–107.
<https://doi.org/10.1016/j.ijantimicag.2011.02.014>
- Hadi, S. M., & Aldujaili, N. H. (2022). Bio-environmental preparation of selenium nanoparticle using **Klebsiella pneumoniae** and their biomedical activity. **IOP Conference Series: Earth and Environmental Science*, 1029*(1), 012021.
<https://doi.org/10.1088/1755-1315/1029/1/012021>
- Han, L., Fu, Q., Deng, C., Luo, L., Xiang, T., & Zhao, H. (2021). Immunomodulatory potential of flavonoids for the treatment of autoimmune diseases and tumour. **Scandinavian Journal of Immunology*, 95*(1), e13106.
<https://doi.org/10.1111/sji.13106>
- Huang, M., Liu, X., Ren, Y., Huang, Q., Shi, Y., Yuan, P., & Chen, M. (2024). Quercetin: A flavonoid with potential for treating acute lung injury. **Drug Design, Development and Therapy*, 18*, 5709–5728.
<https://doi.org/10.2147/dddt.s499037>
- Ismail, T. F., Abdulkareem, S. M., & Jafar, S. N. (2023). Ameliorative potentials of quercetin in some histo-physiological and biochemical parameters against alterations induced by benzene inhalation in albino rats. **Iraqi Journal of Science*, 64*(7), 4151–4162.
<https://doi.org/10.24996/ij.s.2023.64.7.6>
- Li, Y., Yao, J., Han, C., Yang, J., Chaudhry, M. T., Wang, S., Liu, H., & Yin, Y. (2016). Quercetin, inflammation and immunity. **Nutrients*, 8*(3), 167.
<https://doi.org/10.3390/nu8030167>
- Luna, L. G. (1968). **Manual of histologic staining methods of the Armed Forces Institute of Pathology** (5th ed.). McGraw-Hill.
<http://ci.nii.ac.jp/ncid/BA07883946>
- Mohammed, R. J. (2025). The impact of quercetin berberine complex and clove extract on mice induced asthmatic condition. **Agricultural Biotechnology Journal*, 17*(3), 385–406.
<https://doi.org/10.22103/jab.2025.25794.1755>

- Navon-Venezia, S., Kondratyeva, K., & Carattoli, A. (2017). *Klebsiella pneumoniae*: A major worldwide source and shuttle for antibiotic resistance. *FEMS Microbiology Reviews*, 41*(3), 252–275. <https://doi.org/10.1093/femsre/fux013>
- Obead, N. N. K., Arif, N. I. S., & Waheed, H. J. (2025). Effects of different doses of quercetin on apoptotic markers and liver enzymes in liver injury induced by interferon beta-1b (Betaferon) in male rats in comparison with silymarin. *Iraqi Journal of Pharmaceutical Sciences*, 34*(2), 108–115. <https://doi.org/10.31351/vol34iss2pp108-115>
- Qader, G. I., Aziz, R., Ahmed, Z., Abdullah, Z., & Hussain, S. A. (2014). Protective effects of quercetin against isoniazid and rifampicin induced hepatotoxicity in rats. *American Journal of Pharmacological Sciences*, 2*(3), 56–60. <https://doi.org/10.12691/ajps-2-3-3>
- Riwu, K. H. P., Effendi, M. H., Rantam, F. A., Khairullah, A. R., & Widodo, A. (2022). A review: Virulence factors of *Klebsiella pneumoniae* as emerging infection on the food chain. *Veterinary World*, 15*(9), 2172–2179. <https://doi.org/10.14202/vetworld.2022.2172-2179>
- Vithalkar, M. P., Pradhan, S., Sandra, K. S., Bharath, H. B., & Nayak, Y. (2025). Modulating NLRP3 inflammasomes in idiopathic pulmonary fibrosis: A comprehensive review on flavonoid-based interventions. *Cell Biochemistry and Biophysics.* <https://doi.org/10.1007/s12013-025-01696-4>
- Wang, G., Wang, Y., Yao, L., Gu, W., Zhao, S., Shen, Z., Lin, Z., Liu, W., & Yan, T. (2022). Pharmacological activity of quercetin: An updated review. *Evidence-Based Complementary and Alternative Medicine*, 2022*, 3997190. <https://doi.org/10.1155/2022/3997190>
- Zhang, C., Wang, R., Zhang, G., & Gong, D. (2018). Mechanistic insights into the inhibition of quercetin on xanthine oxidase. *International Journal of Biological Macromolecules*, 112*, 405–412. <https://doi.org/10.1016/j.ijbiomac.2018.01.190>